frontiers | Frontiers in Environmental Science

TYPE Original Research
PUBLISHED 17 July 2024
DOI 10.3389/fenvs.2024.1396772

OPEN ACCESS

EDITED BY
Visva Bharati Barua,
University of North Carolina at Charlotte, United States

REVIEWED BY
Arnab Ghosh,
Dong-A University, Republic of Korea
Divya Pal,
Stockholm University, Sweden

*CORRESPONDENCE
Sun Wen,
511058758@qq.com,
imsunwen@gmail.com

RECEIVED 07 March 2024
ACCEPTED 17 May 2024
PUBLISHED 17 July 2024

CITATION
Wen S, Yang Z, Biao P and Jing W (2024), Effect mechanism of nutrients on pathogenic bacteria at the sediment-water interface in eutrophic water.
Front. Environ. Sci. 12:1396772.
doi: 10.3389/fenvs.2024.1396772

Effect mechanism of nutrients on pathogenic bacteria at the sediment-water interface in eutrophic water

Sun Wen[1,2,3]*, Zhang Yang[2,3], Peng Biao[2,3] and Wang Jing[2,3]

[1]Technology Innovation Center for Land Engineering and Human Settlements, Shaanxi Land Engineering Construction Group Co., Ltd., and Xi'an Jiaotong University, Xi'an, China, [2]Key Laboratory of Degraded and Unused Land Consolidation Engineering, Ministry of Natural and Resources of China, Xi'an, China, [3]Shaanxi Provincial Land Engineering Construction Group, Land Engineering Technology Innovation Center, Ministry of Natural Resources, Xi'an, China

This research analyzed the structure of microbial groups in the sediment–water interface (SWI) and the relationship between the gene expression levels of two typical pathogenic bacteria *Escherichia coli* and *Enterococcus*, and nutrient levels using modern biological techniques. The nutrient distribution at the SWI revealed significantly higher nutrient content in the sediment compared to the overlying water. According to Fick's first law, the release flux indicated that PO_4^{3-}-P in the upper reaches of the reservoir was deposited from the overlying water, while the release rate of NH_4^+-N, in addition to sedimentation, was significantly greater than that of PO_4^{3-}P. The microbial community structure was primarily dominated by the genera *Methyloparacoccus*, *Methylomonas*, and *Arenimonas*. The abundances of *E. coli* and *Enterococcus* were higher in the surface sediment than in the overlying water. Pearson correlation analysis demonstrated that *E. coli* had a significant positive correlation with total nitrogen (TN) ($p < 0.05$) and total phosphorus (TP) ($p < 0.05$), whereas *Enterococcus* had a very significant positive correlation with TN and TP ($p < 0.01$).

KEYWORDS

sediment-water interface, nutrients, pathogenic bacteria, correlation, eutrophic water

1 Introduction

Eutrophication in closed water bodies, such as lakes and reservoirs, has become a pollution problem encountered in water environments worldwide. Statistics show (Zhao et al., 2010) that more than 75% of the world's closed water bodies have eutrophication problems. Of the 132 major lakes in China, 61 or 46.21% are eutrophic. The northeast and eastern plain lake areas are more severely eutrophic than other areas, with their eutrophication ratios reaching 66.70% and 53.90%, respectively. Sediment has attracted attention as a main endogenous polluter of lakes and reservoirs. Nitrogen and phosphorus tend to accumulate in sediments (Liu et al., 2012) and can diffuse into the water column through changes in environmental factors, such as hydrodynamic disturbances, temperature fluctuations, and dissolved oxygen (Portielje and Lijklema, 1999), causing secondary pollution. When the nitrogen and phosphorus content in the water column increases to a certain level, algae overgrow, leading to the eutrophication of the water column and posing a severe threat to the ecological environment (Chen et al., 2022). This study

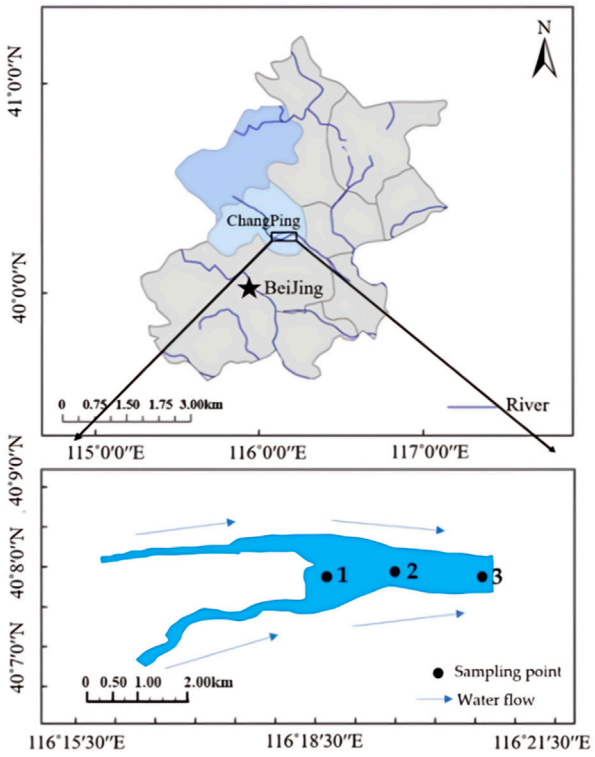

FIGURE 1
Arrangement and zoning map of sampling points in Shahe Reservoir. (The figure wascreated by S.W (Sun et al., 2021), and modifed using ArcGIS sofware 10.2; Source: WGS 1984).

selected the Shahe Reservoir located in Changping District, Beijing, which belongs to the Shahe River Basin. It is mainly recharged by the return water from urban sewage treatment plants, which increases the content of organic matter and nutrients in the reservoir water.

The sediment–water interface (SWI), as one of the most important interfaces in water ecosystems, is a crucial site for controlling material cycling in lakes and reservoirs (Fan, 2019). Nutrient production, cycling, and transfer are exceptionally active at the SWI zone, and most of these processes exert physical, chemical and biological effects on the microscale (millimeter and submillimeter) environment (Fielding et al., 2020). Given that many metabolic processes in reservoirs occur at the SWI and the transport and transformation of contaminants at the SWI is complex. While existing research extensively examines the distribution and release patterns of pollutants at the sediment-water interface, scant attention has been devoted to the presence of pathogenic bacteria. Therefore, this study is dedicated to elucidating the distribution characteristics and release dynamics of nutrients at the sediment-water interface, with a specific focus on their correlation with pathogenic bacteria. By exploring the underlying laws governing these phenomena, this research bears significant theoretical and practical implications for understanding the environmental behavior of pathogenic bacteria (Xu et al., 2013; Lei et al., 2018; Wen et al., 2018).

2 Materials and methods

2.1 Brief mapping of the studied area

The North Canal water system originates from the Southern foot of Yanshan Mountain in Changping District, Beijing, and flows through Beijing, Langfang, Hebei Province and Tianjin, successively (Yang et al., 2012). Shahe Reservoir is an important node located in the source area of the NorthCanal (Figure 1). The drainage area of Shahe Reservoir is about 1,125 km^2, of which the mountain area accountsfor about 75%. Shahe Reservoir is a typical channel-type reservoir in the upper reaches of the North Canal. The water in the Shahe Reservoir area has a long residence time and is a stagnant water body (Yu et al., 2012). The issue of eutrophication in reservoirs has garnered significant attention. Nutrients stored within reservoir sediments posed potential risks of release, thereby serving as a source of endogenous pollution within the reservoir. (Sun et al., 2021).

2.2 Sample collection and processing

Based on their topographical characteristics, three sediment sampling points were set up within the Shahe Reservoir study area (Figure 1). In September 2018, Three columnar sediment samples were collected at sampling points S1,S2, and S3 using a mud core sampler to analyze the vertical distribution characteristics of nutrients and pathogens. (r = 50 mm, h = 60 cm).

The sediment columns were layered at 2 cm intervals, and the layered samples were freeze-dried (Model FD-1A-50 freeze dryer, Beijing Boyikang Experimental Instrument Co., Ltd.), crushed with a glass rod to remove impurities such as gravel, shells, and animal and plant residues, ground with a mortar, and passed through a 100-mesh sieve before analysis. Meanwhile, the samples obtained by the Peterson mud harvester were mixed and put into a 50 mL centrifuge tube, centrifuged at 4,000 rpm for 20 min to obtain interstitial water, and stored at −4 °C. The overlying water was sucked from the gravity column mud extractor by siphon method, put into a 50 mL centrifuge tube, and stored at −4°C (Sun et al., 2022).

Determination of nutrient indicators in interstitial water includes ammonia nitrogen (NH_4^+-N), total nitrogen (TN), orthophosphate (PO_4^{3-}-P) and total phosphorus (TP) (Sun et al., 2021): where TN: interstitial water is diluted to below 4 mg L^{-1}, and after potassium sulfate digestion (Alfa Aesar,United Kingdom), UV spectrophotometer colorimetry is used; TP:The interstitial water is diluted with raw water to below 1.2 mg L^{-1} and after potassium sulfate digestion, molybdenum antimony anti-spectrophotometry is used. NH_4^+-N: After the interstitial water was filtered through a 0.45 μm filter membrane and diluted to diluted to below 2 mg L^{-1}, the Nessler reagent spectrophotometry was used; PO_4^{3-}-P: After the interstitial water was filtered through a 0.45 μm filter membrane and diluted to below 1.2 mg L^{-1}, the molybdenum antimony was used to Anti-spectrophotometry; the instruments used for the measurement are UV-Vis spectrophotometers (TU-1901, Beijing Puxi General Instrument Co., Ltd.)

TABLE 1 Primers and their mechanisms used in this study.

Target genes	Primer	Sequences	Amplico Size (bp)	Annealing Temp (°C)
16 s rRNA	1369F	CGG TGA ATA CGT TCY CGG	128	55
	1492R	GGW TAC CTT GTT ACG ACT T		
Enterococci	ECST784F	AGA AAT TCC AAA CGA ACT TG	93	55
	ENC854R	CAG TGC TCT ACC TCC ATC ATT		
E.coli	23 s rRNA-F	GGT AGA GCA CTG TTT TGG CA	87	60
	23 s rRNA-R	TGT CTC CCG TGA TAA CTT TCTC		

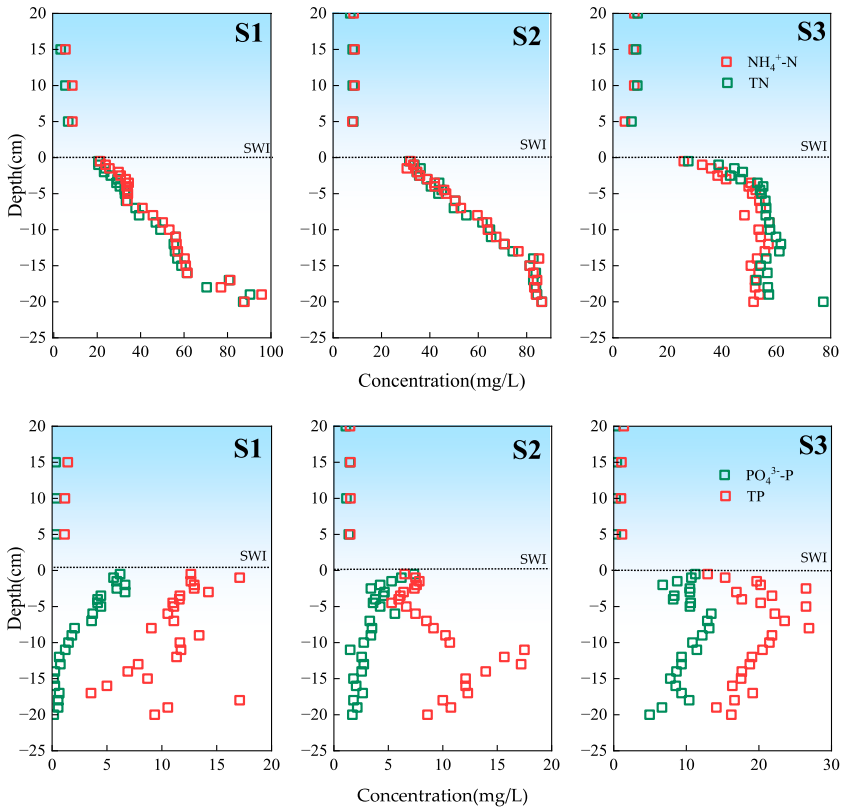

FIGURE 2
Spatial distribution characteristics of NH_4^+-N, TN, $PO4^{3-}$-P and TP at SWI.

2.2.1 DNA extraction

The DNA extraction process involved several steps: Soil samples were crushed into fine particles to aid DNA release. Following the instructions of the FastDNA Spin Kit for Soil (MP Bio, USA), soil samples were added to extraction reagents containing cell lysis agents and proteinase. The samples were thoroughly mixed and briefly centrifuged to pelletize soil particles. The supernatant, containing released DNA, was transferred to a new centrifuge tube. DNA precipitation was achieved by adding an appropriate solution, followed by centrifugation to pelletize DNA. The DNA pellet was washed with 70% ethanol to remove contaminants. After dissolution in provided buffer, DNA concentration and purity were measured using a spectrophotometer. The extracted DNA was then stored at −20°C or −80°Cfor subsequent molecular biology experiments.

2.2.2 Microbial community structure analysis

The gene sequences of the 16S rRNA V4 region PCR products were determined based on high-throughput sequencing, and the microbial community structure in each sample was analyzed. The PCR primer used was 515F/806R, and the barcode sequence was added before the forward primer to distinguish the PCR products from different samples. PCR was repeated three times for each sample and mixed, and then PCR products were recovered from

TABLE 2 Fluxes of NH_4^+-N and PO_4^{3-}P.

Nutrients	Sampling point	Curve fitting	R	$D_s \times 10^{-6}\,(cm^2 \cdot s^{-1})$	$\partial_c / \partial_x mg\,(L \cdot cm)^{-1}$	$Fmg\,(m^2 \cdot d)^{-1}$
NH_4^+-N	S1	y = 17.57e-0.093x	0.97	11.3	−1.63	12.72
	S2	y = 29.578e-0.069x	0.95	11.3	−0.93	7.26
	S3	y = 25.622e-0.06x	0.82	11.3	−1.54	11.97
PO_4^{3-}-P	S1	y = 1.9464e0.0502x	0.33	3.92	0.1	−0.26
	S2	y = 2.7313e-0.005x	0.10	3.92	−0.01	0.03
	S3	y = 3.4611e-0.091x	0.72	3.92	−0.31	0.85

different samples. PCR products were mixed in equal amounts, and libraries were built and sequenced; library building and sequencing were done by Sankyo Bioengineering (Shanghai) Co. The Illumina MiSeq™ platform was employed for sequencing. Primer-linked sequences (TGG AAT TTC TCT GGG TGC CCA AGG AACTC) were initially removed from the MiSeq paired-end sequencing data. Following this, paired reads were merged into single sequences based on their overlap. Samples were then distinguished according to their individual sequences. Finally, the quality of each sample data was controlled and filtered to ensure the validity of the data obtained. (Sun et al., 2021; Wei et al., 2021).

2.2.3 Quantitative PCR (qPCR) analysis

The main reagents used for quantitative PCR (qPCR) analysis in this study were SYBR® Premix Ex Taq™ (Tli RNaseH Plus) (TAKARA) and RNase-free Water (Ambion). The qPCR analysis was carried out on a micro ultraviolet spectrophotometer (Nanodrop 2000) and a fluorescent quantitative PCR instrument (StepOne Plus). The amplification efficiencies of the target gene fragments of *Enterococcus* and *E. coli* were 99.54% and 97.82%, respectively. The specific primer sequences and PCR conditions are shown in Table 1 (Sun et al., 2021).

2.2.4 Calculation of release flux

The presence of nutrients in sediments, acting as endogenous pollution, exerted a significant influence on water bodies and was closely intertwined with nutrient exchange at the SWI (Serruya et al., 1974). The concentration gradient of nutrients between the overlying water and the interstitial water of the sediment facilitated molecular diffusion, resulting in the release of nutrient salts from the interstitial water into the overlying water or their diffusion from the overlying water into the interstitial water. Consequently, investigating the release flux of interfacial nutrients at the SWI was of paramount importance (Huang et al., 2006). According to the concentration gradient of different nutrient concentrations at the SWI of the Shahe Reservoir, and using the one-dimensional pore water diffusion model (Selig et al., 2007) (Fick's law) and related literature (Ullman and Aller, 1982; Mccomb et al., 1998), the endogenous nutrient diffusion flux of the Shahe Reservoir can be estimated, and its improved formula is as follows:

$$F = \varphi \times D_s \times \frac{\partial c}{\partial x} \quad (1)$$

where F indicates diffusion flux at the SWI($mg \cdot m^{-2}\,d^{-1}$);

φ indicates the surface sediment porosity(%);

D_s indicates the actual molecular diffusion coefficient considering the bending effect of the sediment($m^2 \cdot s^{-1}$);

∂_c/∂_x indicates the interface substance concentration gradient($mg \cdot L^{-1}\,cm^{-1}$);

The empirical relationship between D_s and porosity is: $\varphi < 0.7$, $D_s = \varphi \times D_0$; when $\varphi > 0.7$, $D_s = \varphi^2 \times D_0$; D_0 indicates the ideal diffusion coefficient of infinitely diluted solution($cm^2 \cdot s^{-1}$).

2.3 Analysis of microbial community structure and typical, pathogens

Based on metagenomic classification and sequencing, the PCR products of 16S rRNA V4 regions were determined, and the microbial community structure in each sample was analyzed. The PCR for each sample was repeated three times before they were mixed. For this, the PCR products were recovered using gel, and the PCR products from different samples were mixed in equal amounts for library construction and sequencing; library construction and sequencing were completed by related sequencing companies, and the sequencing platform was Illumina Miseq × 250. For Miseq paired-end sequencing data, the primer adapter sequence (TGG AAT TCT CGG GTG CCA AGG AAC TC) needed to be removed first, and then the paired reads were merged into a sequence according to the overlap relationship between paired-end reads. Samples were then identified and distinguished according to the barcode tag sequence. Finally, quality control filtering was performed on the samples to ensure valid data for each sample (Pawlowski et al., 2022).

Following guidance on relevant standards for pathogens in surface waters from the United States Environmental Protection Agency, the European Union, and the World Health Organization, this study selected the typical pathogens *Escherichia coli* and *ENT* for analysis, using their gene copy numbers (DNA copies·g^{-1}) to represent their corresponding content in the sediment, and their proportion (%) in 16S rRNA to represent their abundance.

2.4 Data processing and analysis methods

SPSS 25.0 software was used to analyze the correlation between the pathogens and Nutrients in interstitial water. The vertical spatial distribution of nutrients in the interstitial waterand the absolute content of pathogens(copies·g^{-1}) were analyzed by Origin 2017. The heat map of the microbial community structure in the sediment was

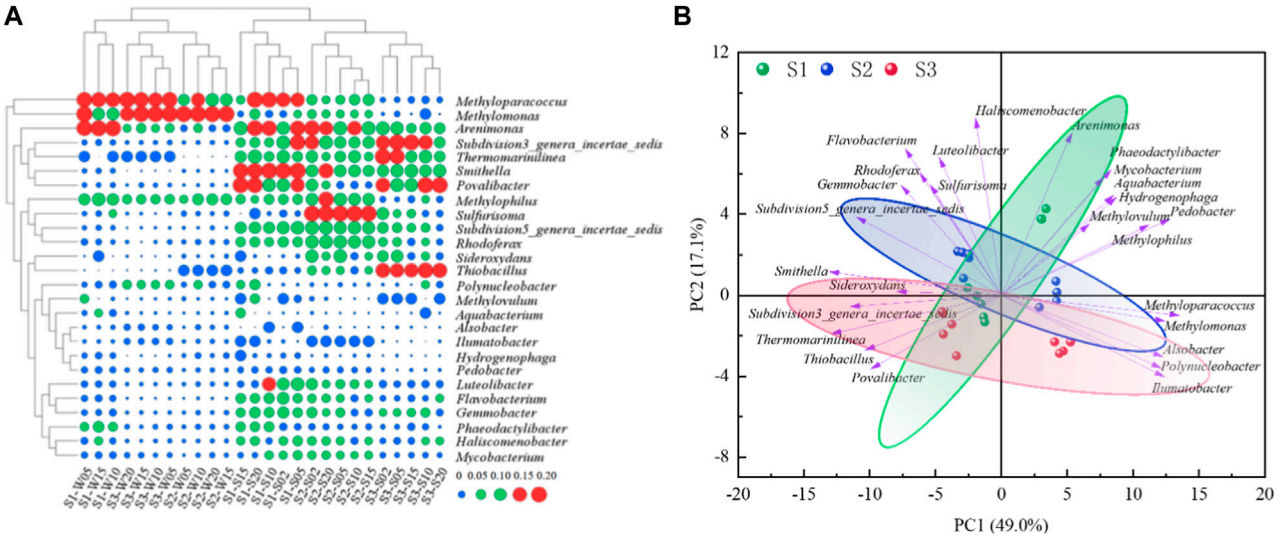

FIGURE 3
(A) SWI community structure diagram(log2 transformed) **(B)** SWI community structure principal component analysis diagram.

constructed using Heml 1.0 (http://hemi.biocuckoo.org/down.php). The R language ade4 package (https://www.R-project.org/.12c) was used to perform noise reduction analysis on operational taxonomic units (OTUs) in the community structure. The average abundance of OTUs in all samples were required to be higher than 0.01%. The OTUs after noise reduction analysis were used for subsequent analysis.

3 Results

3.1 Vertical distribution characteristics of nitrogen nutrients at the SWI

The spatial distribution characteristics of NH_4^+-N and TN at the SWI are shown in Figure 2. At the upstream of the reservoir (S1), the central area of the reservoir (S2), and the downstream of the reservoir (S3) in the overlying water, NH_4^+-N had the same vertical change trend as TN, and its concentration did not change. The concentrations of NH_4^+-N and TN in S1 were 3.20–90.35 and 5.85–95.75 mg·L^{-1}, respectively, with average values of 41.77 ± 23.21 and 44.60 ± 22.86 mg·L^{-1}, respectively. The concentrations of NH_4^+-N and TN in S2 were 9.11–86.35 and 9.32–86.40 mg·L^{-1}, respectively, with average values of 53.18 ± 25.22 and 54.02 ± 25.19 mg·L^{-1}, respectively. The concentrations of NH_4^+-N and TN in S3 were 4.45–57.45 and 6.83–77.30 mg·L^{-1}, respectively, with mean values of 43.09 ± 16.25 and 47.49 ± 17.71 mg·L^{-1}, respectively. With the increase in depth from the SWI downward, the oxygen content in the sediment decreased, the anaerobic environment became conducive to the ammonification of organic nitrogen, and ammonia consumption weakened, resulting in the accumulation of NH_4^+-N in sediments (Shen et al., 2020), These results showed that the concentration of NH_4^+-N increases with depth.

The spatial distribution characteristics of PO_4^{3-}-P and TP at the SWI are shown in Figure 2. In the water overlying S1, S2, and S3, PO_4^{3-}-P and TP exhibited the same vertical change trend and their concentration did not change. However, the concentration of PO_4^{3-}-P and TP in the interstitial water of the sedimentary column at each sampling point gradually increased with the increase in depth. The concentrations of PO_4^{3-}-P and TP in S1 were 0.15–6.65 and 1.31–17.10 mg·L^{-1}, respectively, with the average values of 2.60 ± 2.33 and 10.27 ± 4.42 mg·L^{-1}, respectively. The concentrations of PO_4^{3-}-P and TP in S2 were between 1.10–7.35 and 1.48–17.50 mg·L^{-1}, respectively, with the average values of 3.19 ± 1.57 8.60 ± 4.26 mg·L^{-1}, respectively. The PO_4^{3-}-P and TP concentrations in S3 were 0.26–13.45 and 1.00–26.90 mg·L^{-1}, respectively, with the mean values of 8.50 ± 3.79 and 17.05 ± 7.19 mg·L^{-1}, respectively. Related research (Gong et al., 2017) found that with the strengthening of the reducing environment inside the sediment, Fe^{3+} is continuously reduced into Fe^{2+}, and iron-bound phosphorus is also released such that the release of phosphorus at the SWI increases. Under reducing conditions within sediment, Fe3+ is converted to Fe2+ through reductive dissolution. This process is driven by microbial activity and anaerobic conditions. As Fe3+ is reduced to Fe2+, iron-bound phosphorus is released into the surrounding water. (Ding et al., 2016). At the same time, related works discovered that the secretion of nitrate bacteria (like *Nitrosomonas* and *Nitrobacter)* can accelerate the dissolution of Fe^{3+}, releasing the phosphorus adsorbed by $Fe(OH)_3$ (Jansson, 1986). Therefore, the orthophosphate content at 0–3 cm in the SWI environment showed a gradually decreasing distribution.

The release flux (F) of NH_4^+-N at the SWI is shown in Table 2. Its correlation coefficient in S1, S2, and S3 exceeded 0.80. The exponential fitting curve was ideal. As can be concluded from the value of F, NH_4^+-N at the SWI is released from the sediment in the interstitial water to the overlying water body and sediment is the source of NH_4^+-N. The F of NH_4^+-N ranged from 7.26 mg·m^2·day^{-1} to 12.72 mg·m^2·day^{-1}. NH_4^+-N in the sediment interstitial water enters the overlying water body with the concentration gradient under the action of molecular diffusion; therefore, NH_4^+-N is

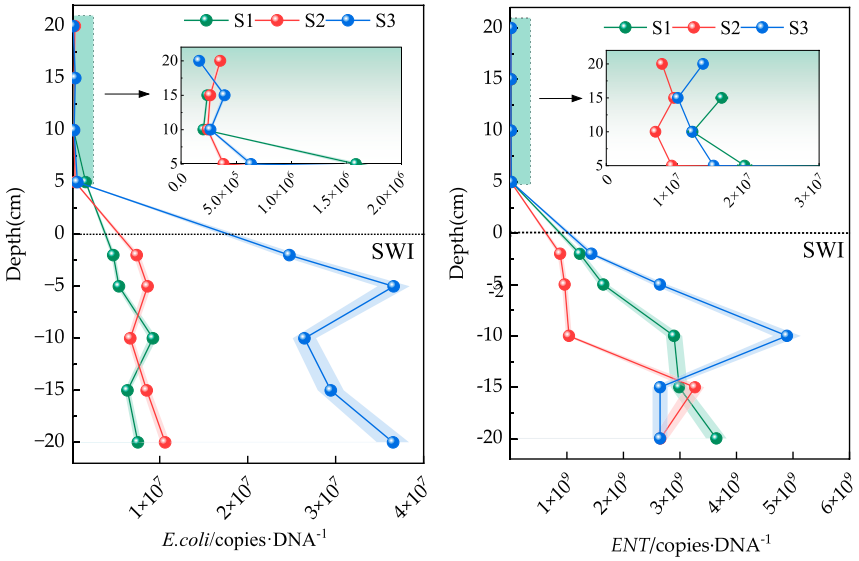

FIGURE 4
Distribution characteristics of *E. coli* and *ENT* in the SWI.

potentially released from the sediment in the interstitial water to the overlying water (Nicholls and Trimmer, 2009). NH_4^+-N had high F in the upper reaches because aquatic plants and phytoplankton utilize NH_4^+-N first when using nitrogen nutrients (Melzer and Melzer, 2004). Most of the NH_4^+-N in interstitial water originates from organic matter decomposition, which regenerates NH_4^+-N (Meng et al., 2020). Moreover, human activities and industrial production in the upper reaches contribute abundant nitrogen nutrients to the upper reaches.

The F value (−0.26 mg m^{-2}·day^{-1}) of PO_4^{3-}-P at the SWI was different from that of NH_4^+-N. PO_4^{3-}-P at the SWI in the upper reaches (S1) is absorbed by sediments. As can be concluded from the F values in S2 and S3, PO_4^{3-}-P at the SWI is released from the sediment in the interstitial water to the overlying water body. The F values in S2 and S3 were 0.03 and 0.85 mg m^{-2}·day^{-1}, respectively. The migration and release of PO_4^{3-}-P at the SWI is affected by many factors (Liu et al., 2018). Li found that under aerobic conditions, the millimeter-scale aerobic layer on the sediment surface and the diffusion boundary layer below the SWI prevent the release of phosphorus in the interstitial water to the overlying water (Li et al., 2016), Moreover, when the dissolved oxygen content in the overlying water decreases, the diffusion boundary layer or aerobic layer becomes thin or disappears, and phosphorus in the interstitial water is released to the overlying water body along the concentration gradient under the action of molecular diffusion (Wang et al., 2010).

The distribution of nutrient content at the SWI mainly shows that the nutrient content in the sediment was significantly greater than that in the overlying water body. The calculation of F in accordance with Fick's first law revealed that only the F value of PO_4^{3-}-P in S1 was negative (−0.26 mg/m^2·day), that is, PO_4^{3-}-P is deposited from the overlying water to the sediment. The release rates of NH_4^+-N in S1, S2, and S3 (12.72, 7.26, and 11.97 mg/m^2·day) were significantly greater than those of PO_4^{3-}-P in S2 and S3 (0.03 and 0.85 mg/m^2·day) because when aquatic plants and phytoplankton use nitrogen nutrients, they first use NH_4^+-N. Moreover, most of the NH_4^+-N in interstitial water originates from the decomposition of organic matter, which regenerates NH_4^+-N. Meanwhile, for PO_4^{3-}-P, the diffusion boundary and aerobic layer in the lower layer of the interface prevent the release of phosphorus in the interstitial water. Moreover, overlying water or the peak concentration of PO_4^{3-}-P in the sediment surface inhibits the migration and release of PO_4^{3-}-P in the lower layer to the upper layer. The F of PO_4^{3-}-P was significantly lower than that of NH_4^+-N.

3.2 Structural characteristics of microbial communities at the SWI

The distribution characteristics of the microbial community structure at the SWI are shown in Figure 3A, the results of principal component analysis are shown in Figure 3B, which shows that the similarities and differences of the microbial community structure at the SWI are reflected in the overlying water bodies and sediments, respectively. *Methyloparacoccus* is a strictly respiratory Gram-negative aerobic genus that uses oxygen as the terminal electron acceptor, and its average relative abundance in the SWI of each sampling point was the highest (13.88% ± 6.30%). Its relative abundance was the highest (23.42%) at the 20 cm layer of the overlying water downstream of the reservoir (3# sedimentation column), and its relative abundance was the lowest (1.58%) at the −2 cm layer of the sediment. The genus *Methylomonas* has a wide distribution and is a chemoorganotrophic bacterium without strict requirements for inorganic nutrients. It may grow on natural substrates containing methane (Tikhonova et al., 2023). Most of its members are symbiotic or associated with heterotrophic bacteria that cannot oxidize methane, and isolating, purifying, and maintaining pure species of this genus are extremely difficult. Trace amounts of organic substances, such as amino acids and polypeptides, can inhibit their growth, and even some methane-oxidizing bacteria are inhibited by very small amounts of methanol.

10.3389/fenvs.2024.1396772

TABLE 3 The Pearson correlation analysis between pathogenic bacteria and TN, TP in the SWI.

Types of pathogens	Pearson correlation	S1 sedimentary column		S2 sedimentary column		S3 sedimentary column	
		TN	TP	TN	TP	TN	TP
E. coli	Correlation coefficient	0.862*	0.830*	0.993*	0.990*	0.972**	0.969**
	Significance	0.027	0.041	0.045	0.045	0.001	0.001
ENT	Correlation coefficient	0.996**	0.999**	0.981	0.977	0.981**	0.983**
	Significance	0.00003	0.000	0.123	0.136	0.001	0.0004

Some bacteria are strictly aerobic, using oxygen molecules as electron acceptors to oxidize methane gradually into alcohols, aldehydes, acids, and finally into carbon dioxide, and obtain energy through the monophosphate ribose or serine pathway (Khalifa et al., 2015). The average relative abundance of *Methylomonas* at the SWI was 13.60% ± 8.55% and was second only to that of *Methyloparacoccus*. It was highest (28.24%) at the 5 cm layer of the overlying water in S2 and lowest (2.12%) at the −2 cm layer of S1. The average abundances of *Arenimonas* and *Methylophilus* at the SWI at each sampling point were also relatively high, reaching 9.57% ± 3.46% and 7.94% ± 2.26%, respectively. The maximum values appeared at 10 (14.54%) and 15 cm (9.66%) of S1, and the smallest values were distributed at 5 cm of the upper water in S2 (5.79%) and the −2 cm layer of sediment in S3 (1.96%). The average abundances of *Polynucleobacter, Phaeodactylibacter, Sulfurisoma*, and *Subdivision3_genera_incertae_sedis* at the SWI at each sampling point exceeded 3.00%. The maximum abundances of *Phaeodactylibacter* and *Sulfurisoma* were 7.20% and 8.84%, respectively, and appeared at 20 cm above S1. The maximum abundance of *Subdivision3_genera_incertae_sedis* was 9.44% and was found at the −2 cm sediment layer in S3. The minimum abundances of *Polynucleobacter* and *Phaeodactylibacter* were 0.55% and 1.32%, respectively, and appeared at the −2 cm layer in S3. The minimum abundance of *Sulfurisoma* was 0.64% and appeared at the 10 cm layer of the overlying water of S3. The minimum value of *Subdivision3_genera_incertae_sedis* was 1.69% and was found at the 25 cm layer of the overlying water of S3.

3.3 Relative abundance of pathogenic bacteria in the SWI

The absolute abundance distribution of *E. coli* and *Enterococcus* at the SWI is shown in Figure 4. Given that the sediment layer in S3 was relatively high, the overlying water body was only sampled to 10 cm above the surface sediment. The figure shows that the absolute abundance ranges of *E. coli* in S1, S2, and S3 were 2.03×10^5–4.72×10^6, 2.41×10^5–7.39×10^6 and 2.20×10^5–2.47×10^7 copies·g^{-1}, respectively. The absolute abundance of *E. coli* at the SWI negligibly differed. Notably, the absolute abundance of *E. coli* in the surface layer of the SWI at the −2 cm sediment layer in the three sedimentary columns was one order of magnitude higher than that in the overlying water body. Although the absolute abundance of *E. coli* at the SWI in the overlying water showed little difference, that at 20 cm above the SWI in S1 and S3 was slightly higher than that at other depths of overlying water.

The distribution characteristics of the absolute abundances of *Enterococcus* and *E. coli* at the SWI were not considerably different and were both higher in sediment than in the overlying water body. However, the absolute abundance of *Enterococcus* at the SWI was approximately two orders of magnitude higher than that of *E. coli*. *Enterococcus* species are known for their resilience and ability to survive in harsh environmental conditions, including low nutrient environments and fluctuating temperatures. They can form biofilms and persist in sediments for extended periods, enhancing their abundance at the SWI compared to *E. coli*, which

may be less adapted to such conditions. The absolute abundance ranges of *Enterococcus* in S1, S2, and S3 were 6.30×10^6–1.23×10^9, 6.94×10^6–8.81×10^8 and 8.28×10^6–1.43×10^9, respectively. The abundance of *Enterococcus* in S3 was approximately 1.60 and 1.37 times that in the sedimentation columns in S2 and S1, respectively. The absolute abundance of *Enterococcus* at the SWI was not significantly different. Similar to that of *E. coli*, the absolute abundance of *Enterococcus* in the three sediment columns was approximately one order of magnitude higher than that in the surface −2 cm sediment in the SWI than in the overlying water.

Table 3 shows that *E. coli*, *ENT*, TN, and TP in the SWI in S1 and S3 had extremely significant positive correlations ($p < 0.01$) or significant positive correlations ($p < 0\ .05$). Specifically, *E. coli* had a positive correlation with TN and TP ($p < 0.05$) at the SWI in S1, whereas *ENT* at the SWI in S1 had extremely significant positive correlations with TN and TP ($p < 0.01$). However, the correlation of *Enterococcus* with TN and TP in the SWI in S2 was not significant ($p > 0.05$). *Enterococcus* had extremely significant positive correlations with TN and TP ($p < 0.01$) at the SWI in S3. Relevant studies (Xiang et al., 2023) have found that nitrite can effectively improve denitrification efficiency and enrich bacteria during the nitrification and denitrification processes. Therefore, ammonia can be regarded as one of the pathogenic bacteria pollution source parameters.

4 Conclusion

The distribution of nutrient content at the SWI of the Shahe Reservoir mainly revealed that nutrient content in the sediment was significantly greater than that in the overlying water body. The F values calculated in accordance with Fick's first law showed that the F value of PO_4^{3-}-P was negative only in S1, that is, sediment is deposited from the overlying water. The release rate of NH_4^+-N in S1, S2 and S3 was significantly greater than that of PO_4^{3-}-P in S2 and S3.

The horizontal community structure of pathogenic bacteria at the SWI of Shahe Reservoir was mainly dominated by three genera, namely, *Methyloparacoccus*(13.88%), *Methylomonas*(13.60%), *Arenimonas* (9.57%), *Sulfurisoma*(8.84%) and *Methylophilus*(7.94%).

Pearson correlation analysis showed that at the SWI, *E. coli* had a significant positive correlation with TP and TN ($p < 0.05$), where as *Enterococcus* had a very significant positive correlation with TP and TN ($p < 0.01$).

In conclusion, this study illuminates nutrient dynamics and microbial communities at the sediment–water interface (SWI) of Shahe Reservoir. It underscores sediment's role as a nutrient reservoir, impacting water quality and ecosystem health. Identification of dominant pathogenic bacteria highlights potential public health risks. Future research should explore mechanisms driving nutrient release and microbial dynamics at SWI, considering seasonal variations and anthropogenic influences. Integrated approaches combining metagenomics, geochemistry, and hydrology are crucial for comprehensive understanding and informing sustainable management strategies. This work is vital amid increasing pressures from urbanization, agriculture, and climate change, offering insights for effective water quality preservation and public health safeguarding.

Data availability statement

The original contributions presented in the study are included inthe article/Supplementary Material, further inquiries can be directedto the corresponding authors.

Author contributions

SW: Conceptualization, Writing–original draft, Writing–review and editing. ZY: Investigation, Writing–original draft, Writing–review and editing. PB: Investigation, Resources. WJ: Validation, Software. All authors contributed to the article and approved the submitted version.

Funding

The author(s) declare that financial support was received for the research, authorship, and/or publication of this article. This work was supported by (Shaanxi Key Laboratory of Land Consolidation Open Fund) [Grant number (300102353506)] and (The project of Shaanxi Province Land Engineering Construction Group) [Grant number (DJTD 2023-02) and (DJTD 2022-04)].

Conflict of interest

Author SW was employed by Shaanxi Land Engineering Construction Group Co., Ltd.

The remaining authors declare that the research was conducted in the absence of any commercial or financial relationships that could be construed as a potential conflict of interest.

Publisher's note

References

Chen, T., Liu, C. Q., Shi, X. L., Li, Y., Fan, Z. W., Jia, B. Y., et al. (2022). Ten-year trend analysis of eutrophication status and the related causes in lake hongze. *Environ. Sci.* 43 (7), 3523–3531. doi:10.13227/j.hjkx.202110006

Ding, S., Wang, Y., Wang, D., Li, Y. Y., Gong, M., and Zhang, C. (2016). *In situ*, high-resolution evidence for iron-coupled mobilization of phosphorus in sediments. *Sci. Rep.* 6 (1), 24341. doi:10.1038/srep24341

Fan, C. (2019). Advances and prospect in sediment-water interface of lakes: a review. *J. Lake Sci.* 31 (5), 1191–1218. doi:10.18307/2019.0514

Fielding, J. J., Croudace, I. W., Kemp, A. E., Pearce, R. B., Cotterill, C. J., Langdon, P., et al. (2020). Tracing lake pollution, eutrophication and partial recovery from the sediments of Windermere, UK, using geochemistry and sediment microfabrics. *Sci. total Environ.* 722, 137745. doi:10.1016/j.scitotenv.2020.137745

Gong, M., Zengfeng, J., Yan, W., Juan, L., and Shiming, D. (2017). Coupling between iron and phosphorus in sediments of shallow lakes in the middle and lower reaches of Yangtze River using diffusive gradients in thin films (DGT). *J. Lake Sci.* 29, 1103–1111. doi:10.18307/2017.0508

Huang, X., Guo, F., and Yue, W. (2006). Studies on nutrients in sediment interstitial water in northern South China Sea. *J. Trop. Oceanogr.* 25 (5), 43–48. doi:10.3969/j.issn.1009-5470.2006.05.008

Jansson, M. (1986) *Nitrate as a catalyst for phosphorus mobilization in sediments*. New York: Springer.

Khalifa, A., Lee, C. G., Ogiso, T., Ueno, C., Dianou, D., Demachi, T., et al. (2015). Methylomagnum ishizawai gen. nov., sp. nov., a mesophilic type I methanotroph isolated from rice rhizosphere. *Int. J. Syst. Evol. Microbiol.* 65 (10), 3527–3534. doi:10.1099/ijsem.0.000451

Lei, P., Hong, Z., Chao, W., and Ke, P. (2018). Migration and diffusion for pollutants across the sediment - water interface in lakes, a review. *Environ. Res.* 30 (6), 1489–1508. doi:10.18307/2018.0602

Li, H., Song, C. L., Cao, X. Y., and Zhou, Y. Y. (2016). The phosphorus release pathways and their mechanisms driven by organic carbon and nitrogen in sediments of eutrophic shallow lakes. *Sci. Total Environ.* 572, 280–288. doi:10.1016/j.scitotenv.2016.07.221

Liu, C., Gu, X., Chen, K., Fan, C., Zhang, L., and Huang, W. (2018). Nitrogen and phosphorus exchanges across the sediment–water interface in a bay of lake chaohu. *Water Environ. Res.* 90 (11), 1956–1963. doi:10.2175/106143017x15131012188079

Liu, J., Zheng, X., Chen, L., Wu, C., et al. (2012). Study on flux and release law of nitrogen and phosphorus of sediment in reservoir. *J. Hydraulic Eng.* 43 (3), 339–343.

Mccomb, A. J., Qiu, S., Lukatelich, R., and McAuliffe, T. (1998). Spatial and temporal heterogeneity of sediment phosphorus in the peel-harvey estuarine system. *Estuar. Coast. Shelf Sci.* 47 (5), 561–577. doi:10.1006/ecss.1998.0389

Melzer, S. A., and Melzer, A. (2004). Sediment and water nutrient characteristics in patches of submerged macrophytes in running waters. *Hydrobiologia* 527, 195–207. doi:10.1023/b:hydr.0000043301.50788.36

Meng, X., Zhang, W., and Shan, B. (2020). Distribution of nitrogen and phosphorus and estimation of nutrient fluxes in the water and sediments of Liangzi Lake, China. *Environ. Sci. Pollut. Res. Int.* 27 (7), 7096–7104. doi:10.1007/s11356-019-07398-8

Nicholls, J. C., and Trimmer, M. (2009). Widespread occurrence of the anammox reaction in estuarine sediments. *Aquat. Microb. Ecol.* 55, 105–113. doi:10.3354/ame01285

Pawlowski, J., Bruce, K., Panksep, K., Aguirre, F., Amalfitano, S., Apothéloz-Perret-Gentil, L., et al. (2022). Environmental DNA metabarcoding for benthic monitoring: a review of sediment sampling and DNA extraction methods. *Sci. Total Environ.* 818, 151783. doi:10.1016/j.scitotenv.2021.151783

Portielje, R., and Lijklema, L. (1999). Estimation of sediment–water exchange of solutes in Lake Veluwe, The Netherlands. *Water Res.* 33 (1), 279–285. doi:10.1016/s0043-1354(98)00202-4

Selig, U., Berghoff, S., and Schubert, H. (2007). Transformation of particulate phosphorus at the sediment-water interface in a shallow coastal water on the Baltic Sea. *Int. Assoc. Theor. Appl. limnoloy* 30 (2), 235–238. doi:10.1080/03680770.2008.11902116

Serruya, C., Edelstein, M., Pollingher, U., and Serruya, S. (1974). Lake Kinneret sediments: nutrient composition of the pore water and mud water exchanges 1. *Limnol. Oceanogr.* 19 (3), 489–508. doi:10.4319/lo.1974.19.3.0489

Shen, L. Q., Amatulli, G., Sethi, T., Raymond, P., and Domisch, S. (2020). Estimating nitrogen and phosphorus concentrations in streams and rivers, within a machine learning framework. *Sci. Data* 7 (1), 161. doi:10.1038/s41597-020-0478-7

Sun, W., Yang, K., Li, R., Chen, T., Xia, L., Sun, X., et al. (2022). Distribution characteristics and ecological risk assessment of heavy metals in sediments of Shahe reservoir. *Sci. Rep.* 12 (1), 16239. doi:10.1038/s41598-022-20540-w

Sun, W., Yang, K., Li, R., Chen, T., Xia, L., Wang, Z., et al. (2021). The spatial distribution characteristics of typical pathogens and nitrogen and phosphorus in the sediments of Shahe reservoir and their relationships. *Sci. Rep.* 11 (1), 21745. doi:10.1038/s41598-021-01252-z

Tikhonova, E. N., Suleimanov, R. Z., Miroshnikov, K. K., Oshkin, I. Y., Belova, S. E., Danilova, O. V., et al. (2023). Methylomonas rapida sp. nov., a novel species of fast-growing, carotenoid-producing obligate methanotrophs with high biotechnological potential. *Syst. Appl. Microbiol.* 46 (2), 126398. doi:10.1016/j.syapm.2023.126398

Ullman, W. J., and Aller, R. C. (1982). Diffusion coefficients in nearshore marine sediments. *Limnol. Oceanogr.* 27 (3), 552–556. doi:10.4319/lo.1982.27.3.0552

Wang, J., Shen, J., Zhang, L., Fan, C., Li, W., Pan, J., et al. (2010). Sediment-water nutrient fluxes and the effects of oxygen in lake dianchi and lake Fuxian,Yunnan Province. *J. Lake Sci.* 22 (5), 640–648. doi:10.18307/2010.0503

Wei, Y., Chang, G., Wu, J., Lin, J., Jiang, H., Wang, P., et al. (2021). Preface: special issue on water quality improvement and ecological restoration for river replenished with reclaimed water based on "Source-Flow-Sink" concept. *Acta Sci. Circumstantiae* 41 (1), 1–6.

Wen, S., Gong, W. Q., Wu, T., Zheng, X. L., Jiang, X., Li, X., et al. (2018). Distribution characteristics and fluxes of nitrogen and phosphorus at the sediment-water interface of yuqiao reservoir. *Environ. Sci.* 39 (5), 2154–2164. doi:10.13227/j.hjkx.201709081

Xiang, Y., Zhou, T., Deng, S., Shao, Z., Liu, Y., He, Q., et al. (2023). Nitrite improved nitrification efficiency and enriched ammonia-oxidizing archaea and bacteria in the simultaneous nitrification and denitrification process. *Statements Declar. Water Res. X* 21, 100204. doi:10.1016/j.wroa.2023.100204

Xu, D., Chen, Y., Ding, S., Sun, Q., Wang, Y., and Zhang, C. (2013). Diffusive gradients in thin films technique equipped with a mixed binding gel for simultaneous measurements of dissolved reactive phosphorus and dissolved iron. *Environ. Sci. Technol.* 47 (18), 10477–10484. doi:10.1021/es401822x

Yang, Y., Wei, Y., Zheng, X., Wang, Y., Yu, M., Xiao, Q., et al. (2012). Investigation of microbial contamination in wenyu river of beijing. *Acta Sci. Circumstantiae* 32 (1), 9–18.

Yu, D., Yu, M., Wei, Y., Wang, Y., Zheng, X., Yang, Y., et al. (2012). Spatio-temporal evolution of water environment quality in Wenyu River during 1980—2010. *Acta Sci. Circumstantiae* 32 (11), 2803–2813.

Zhao, Y., Deng, X., Zhan, J., Xi, B., and Li, Q. (2010). Progress on preventing and controlling strategies of lake eutrophication in China. *Environ. Sci. Technol.* 33, 92–98.